Rigid templating of high surface-area, mesoporous, nanocrystalline rutile using a polyether block amide copolymer template†

Xingmao Jiang[ab] and C. Jeffrey Brinker*[bcd]

Received 13th May 2010, Accepted 2nd July 2010
DOI: 10.1039/c0cc01394c

Highly crystalline rutile with a specific surface area as high as 280 m^2 g^{-1} and well-connected uniform mesoporosity has been synthesized by rigid templating using commercial, low-cost polyether block amide. This general, simple synthesis route for high surface-area mesoporous nanocrystalline oxides and nanocomposite membranes is important for catalysis, sensors, energy storage, solar cells, heavy metal removal and separations.

High surface-area crystalline metal oxides with well connected nanopores are needed for improved performance of catalysts, adsorbents, dye-sensitized solar cells, sensors, lithium-ion batteries *etc.*[1] Among candidate materials, titania has been extensively used due to its superior physical and chemical properties for photocatalysis,[2] antimicrobial activity[3] and heavy metal[4] and NO_X removal.[5] Beck and Siegel[6] demonstrated that nanophase rutile TiO_2 is a preferable catalyst for disassociating H_2S above 250 °C. Developing high surface area bulk porous nanocrystalline rutile with good pore accessibility is crucial for the recovery of hydrogen and sulfur and for further hydrogen energy exploitation. Currently, commercial titania nanoparticles are manufactured mainly by flame spray pyrolysis.[7] The surface area is only ~50 m^2 g^{-1}. High surface area rutile is much less available than anatase. Additionally, the nanoparticles need to be pelletized to reduce the pressure drop of fixed bed reactors or for applications where they need to be recycled from liquid medium for multiple uses.[4] Various surfactants and amphiphilic block copolymers such as pluronic block copolymers have been used to direct the assembly of an initially homogeneous solution into various periodic bicontinuous metal oxide/liquid crystal mesophases.[8,9] Conventional thermal treatments used to convert the amorphous mesophase into the desired crystalline phase are normally accompanied by rapid crystallite growth and a significant decrease in surface area. Relaxation of the rubbery chains in the pluronic copolymers allows relatively "free" mass transport of the metal oxide species and consequently fast metal oxide growth. Unconfined or less confined epitaxial growth of nanocrystallites distorts or even blocks the pores. To address this issue high glass transition temperature (T_g) block polymers such as polystyrene-*b*-poly(ethylene oxide) and poly(ethylene-*co*-butylene)-*b*-poly(ethylene oxide) have been used,[10] but their high cost precludes industrial applications. Carbon nanospheres, calcium carbonate, polystyrene and silica beads have been thoroughly investigated as sacrificial templates,[11] but the templates need to be removed by solvent extraction or high-temperature calcination. Further, the embedded isolated nanoparticle templates are difficult to remove from the crystalline oxides. Other rigid, high T_g templates such as polyamide and polyethersulfone only result in limited surface area.[12]

Pebax®, the commercial copolymer poly-(ether block amide), is low-cost, thermally stable and has a hydrophobic crystalline polyamide (PA) hard domain dispersed within a soft hydrophilic polyether matrix.[13] Due to good mechanical strength and thermal stability, along with enhanced permeability and selectivity, various metal oxide nanoparticles have been used as fillers in Pebax membranes for various separations.[14–19]

Here we demonstrate a one-step solvothermal method,[20] using Pebax® 2533 as the template, for synthesis of high surface-area, highly crystalline mesoporous rutile. Pebax 2533 was generously provided by Arkema Inc. 50 g Pebax 2533 was added into 200 g anhydrous isopropanol. The mixture was stirred at 50 °C overnight. 1.0 g $TiCl_4$ and 1.5 g tetraisopropyl titanate (TIPT) were quickly added into 5.5 g of the viscous Pebax solution under nitrogen at room temperature. After stirring over 1 h, the homogeneous solution was put into a solvothermal Parr bomb and kept at 150 °C over 75 h, promoting hydrolysis and condensation reactions of the titanate precursors and resulting in a transparent titania/Pebax monolith. The monolith was washed using 30 ml isopropanol at 50 °C for 5–6 times to extract Pebax which can be recycled. After vacuum drying, the washed monolith gel cracked into a fine powder. Thermogravimetric/differential thermal analysis (TGA/DTA) of the washed rutile sample showed a weight loss of only 0.25% at 450 °C (Fig. S1, ESI†).

For highly reactive metal oxide precursors, nonaqueous solution routes to nanostructured metal oxides are preferable to aqueous sol–gel processes, offering advantages of easy control of sol–gel kinetics, self-assembly and crystal growth, and high crystallinity at low synthesis-temperature.[21] Under solvothermal conditions, metal halides, crystalline titania, or γ-alumina are Lewis acid catalysts[22] for alcohol dehydration, and the hydrolysis of $TiCl_4$ and TIPT is well controlled. The $TiCl_4$/TIPT ratio, solvothermal temperature, Pebax/Ti ratio and alcohol dehydration rate can be used in combination to control sol–gel reactions, the phase and the crystallite size. If TIPT is used as the sole titanium precursor, only amorphous titania is formed at a synthesis temperature of ~150 °C, a

[a] *Aerosol and Respiratory Dosimetry Program, Lovelace Respiratory Research Institute, Albuquerque, NM 87108, USA*
[b] *Center for Micro-Engineered Materials, the University of New Mexico, Albuquerque, NM 87131, USA*
[c] *Sandia National Laboratories, MS 1349, Albuquerque, NM 87106, USA. E-mail: cjbrink@sandia.gov; Fax: +1 505-272-7336; Tel: +1 505-272-7627*
[d] *Departments of Molecular Genetics and Microbiology, University of New Mexico, USA*

† Electronic supplementary information (ESI) available: TGA analysis of rutile sample, low angle XRD for Pebax 2533, and TEM image for Os doped PEBAX film. See DOI: 10.1039/c0cc01394c

higher temperature (~220 °C) and longer synthesis time are required for formation of anatase phase. With increased $TiCl_4$/TIPT ratio, anatase phase or a mixture of anatase and rutile is obtained. When the acidity or the $TiCl_4$/TIPT ratio is high, the solution contains a large amount of $[Ti(OH)Cl_3(OH_2)_2]$ complex monomers,[23] and only rutile crystallites are developed. Through non-covalent bonds with ether groups the titanium species condense, nucleate, and organize into well distributed bicontinuous polyamide and mixed highly crystalline rutile/polyether mesophases. The polarity and hydrogen bonding of regularly repeating amide groups greatly enhance inter-molecular forces, promoting crystallinity and good mechanical properties.[13] Rigid PA domains (melting point for PA: ~200 °C) act as mass transport barriers and confine the crystallization within the hydrophilic domains. Both our simulations[24] and experiments show that sluggish mass transport (high PEBAX concentration, high viscosity, low synthesis temperature) favors multiple localized nucleation events and therefore promotes smaller, uniform nanocrystallites with high surface area. X-Ray diffraction (XRD) analysis (Fig. 1) proves the crystalline titania to be pure single phase rutile. The size of the rutile is estimated to be ~5.0 nm based on Sherrer's equation. It agrees well with the transmission electron microscopy (TEM) (Fig. 2) results and specific surface area data (see below).

The nitrogen sorption isotherm (Fig. 3) is type IV, featuring a hysteresis loop generated by the capillary condensation in mesopores. The Brunauer–Emmet–Teller (BET) specific surface area for the porous rutile is as high as 280 $m^2\ g^{-1}$. The pore size distribution is narrow (inset in Fig. 3). The Frenkel–Halsey–Hill (FHH) fractal dimension is 2.84 at high relative N_2 pressure, indicating a 3-D well-connected

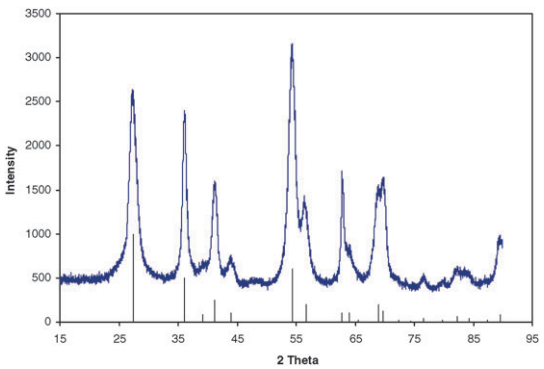

Fig. 1 Wide-angle XRD pattern for washed mesoporous rutile.

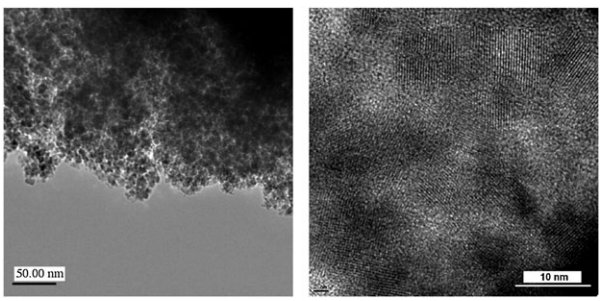

Fig. 2 TEM images of crushed mesoporous rutile. High resolution TEM (right) shows highly crystalline nano rutile.

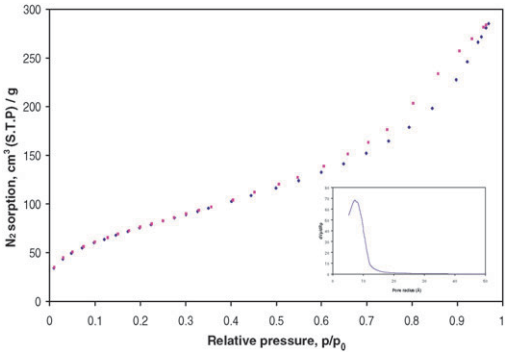

Fig. 3 N_2 sorption isotherm for prepared rutile.

mesoporous network. It is expected that higher surface area can be obtained as a result of reduced rutile crystallite size when the Pebax/Ti ratio in the precursor is increased.

To further clarify the templating process, a Pebax 2533–isopropanol solution was spin-coated on a silicon wafer at 2000 rpm for over 20 s. Low angle XRD of the spin-coated Pebax 2533 film (Fig. S2, ESI†) indicates short range ordering with a characteristic length scale of ~6.7 nm for the phase-separated mesostructure. The Pebax film was then dipped overnight in $OsCl_3$ solution (3.9 mg $OsCl_3$ in 8.0 g DI water). As shown in the TEM image (Fig. S3, ESI†) for the stained Pebax film, hydrophilic polyether domains (dark) are periodically distributed within the hydrophobic rigid polyamide domains (bright). The hydrophilic domain size is ~5.6 nm. The final rutile mesostructure (Fig. 2) mimics the Pebax template (Fig. S3, ESI†), and the pore size of the rutile sample is comparable to the domain sizes of the template, Pebax 2533.

It is expected that this templating method can be applied to the synthesis of high surface area anatase, rutile, and brookite or their mixed phases by varying titanium precursor type, Cl : Ti ratio[25] in the precursor and the solvothermal temperature. The formation of different TiO_2 polymorphs depends on the thermodynamic equilibrium of coexisting soluble octahedral hydroxochloro complexes of the type $[Ti(OH)_aCl_b(OH_2)_c]^{(4-a-b)+}$ where $a + b + c = 6$, and a and b depend on the acidity and the concentration of Cl^- in the solution.[23] The Cl : Ti ratio is the key factor in controlling the acidity and alcohol dehydration rate and determining the particle sizes, the crystalline phases and their relative proportions.[23,25] Compared to $TiCl_4$, $TiOSO_4$ and titanium sulfate favor formation of the $[Ti(OH)_2SO_4(H_2O)_2]$ complex and the condensation of opposed coplanar edges into an anatase type structure.[26]

We further investigated the thermal stability of the rutile sample. As shown in Fig. 4, the mesoporous rutile is stable to annealing to 400 °C for 52.5 h or to 500 °C over 4 h. During high-temperature annealing, rutile nanocrystallites grow due to thermal ripening.

The one-step method is simple, non-destructive, and easy to scale up. By varying the monomeric block types and ratios in the polyether block amide copolymer a wide range of physical and mechanical properties has been achieved.[13] There is available a series of Pebax® with a wide range of polyether and polyamide compositions and polymer chain lengths. This should allow the pore size and surface area to be adjusted by the Pebax type, composition and polyether chain length, and

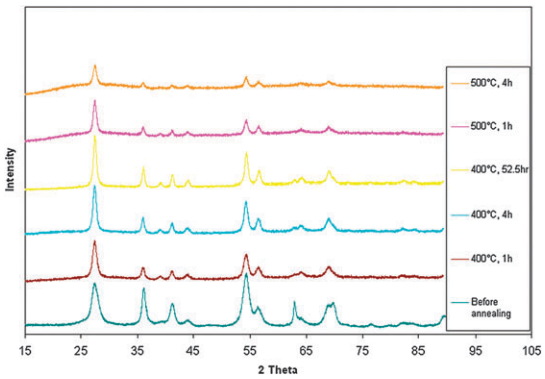

Fig. 4 XRD patterns for mesoporous rutile samples after various annealing.

the relative amount of the block polymer in the precursor. Other block polymers of similar structure can be used, and this general method can be easily extended for other high surface area nanocrystalline metal oxides or metal oxide mixtures for catalysis, adsorption, heavy metal removal, photooxidation, and sensors *etc*. Moreover, this method provides a novel way for fabricating nanocomposite Pebax hybrid membranes with well dispersed nanocrystalline metal oxide or metals of controlled phase and size. The preferential growth and excellent dispersion of the nanocrystalline metal oxide in the hydrophilic polyether domains will reduce the crystallinity of polyether domains and may also increase the free volume,[27] favoring permeation of penetrant molecules in the rubbery polyether matrix. Enhanced permeation and selective sorption of olefins and acid gases on the nanocrystalline metal or metal oxide nanoparticles, combined with good mechanical properties and thermal stability, suggests potential applications of the Pebax membrane as a next generation high-performance nanocomposite membrane for olefin/paraffin, benzene–cyclohexane, and acid gas separation.

This work is supported by the DOE Basic Energy Sciences grant DE-FG02-02-ER15368 (UNM) and the DOE BES Division of Materials Sciences and Engineering (Sandia National Laboratories) and by the National Science Foundation and the Environmental Protection Agency under Cooperative Agreement Number EF 0830117. Sandia is a multiprogram laboratory operated by Sandia Corporation, a Lockheed Martin Company, for the United States Department of Energy's National Nuclear Security Administration under contract DE-AC04-94AL85000.

Notes and references

1 D. L. Li, H. S. Zhou and I. Honma, *Nat. Mater.*, 2004, **3**, 65–72; T. Waitz, M. Tiemann, P. J. Klar, J. Sann, J. Stehr and B. K. Meyer, *Appl. Phys. Lett.*, 2007, **90**, 123108.
2 J. Sun, L. Gao and Q. Zhang, *J. Am. Chem. Soc.*, 2003, **86**, 1677–1682.
3 D. M. Blake, P. C. Maness, Z. Huang, E. J. Wolfrum, J. Huang and W. A. Jacoby, *Sep. Purif. Methods*, 1999, **28**, 1–50.
4 www.dowwatersolutions.com.
5 V. I. Parvulescu, P. Grange and B. Delmon, *Catal. Today*, 1998, **46**, 233–316.
6 D. D. Beck and R. W. Siegel, *US Patent* 5547649, 1996.
7 H. Keskinen, J. M. Mäkelä, S. Hellsten, M. Aromaa, E. Levänen and T. Mäntylä, EUROCVD-15, *Proc. - Electrochem. Soc.*, 2005, **9**, 491–498.
8 J. S. Beck, J. C. Vartuli, W. J. Roth, M. E. Leonowicz, C. T. Kresge, K. D. Schmitt, C. T-W. Chu, D. H. Olson, E. W. Sheppard, S. B. McCullen, J. B. Higgins and J. L. Schlenkert, *J. Am. Chem. Soc.*, 1992, **114**, 10834–10843.
9 G. J. D. A. Soler-Illia, E. L. Crepaldi, D. Grosso and C. Sanchez, *Curr. Opin. Colloid. Interface Sci.*, 2003, **8**, 109–126; D. Zhao, J. Feng, Q. Huo, N. Melosh, G. H. Fredrickson, B. F. Chmelka and G. D. Stucky, *Science*, 1998, **279**, 548–552; S. H. Tolbert, A. Firouzi, G. D. Stucky and B. F. Chmelka, *Science*, 1997, **278**, 264–268.
10 K. Yu, C. Bartels and A. Eisenberg, *Langmuir*, 1999, **15**, 7157–7167; B. Smarsly and M. Antonietti, *Eur. J. Inorg. Chem.*, 2006, 1111–1119.
11 S. H. Park and Y. N. Xia, *Adv. Mater.*, 2000, **10**, 1045–1048.
12 J. H. Schattka, E. H. M. Wong, M. Antonietti and R. A. Caruso, *J. Mater. Chem.*, 2006, **16**, 1414–1420.
13 http://www.arkema-inc.com/index.cfm?pag = 105.
14 R. W. Baker and K. A. Lokhandwala, *US Patent* 5556449, 1996.
15 R. A. Zoppi, S. das Neves and S. P. Nunes, *Polymer*, 2000, **41**, 5461–5470.
16 J. H. Kim and Y. M. Lee, *J. Membr. Sci.*, 2001, **193**, 209–225.
17 S. Sridhar, T. M. Aminabhavi, S. J. Mayor and M. Ramakrishna, *Ind. Eng. Chem. Res.*, 2007, **46**, 8144–8151.
18 J. Müller, K.-V. Peinemann and J. Müller, *Desalination*, 2002, **145**, 339–345.
19 Z. L. Xu, L. Y. Yu and L. F. Han, *Front. Chem. Eng. China*, 2009, **3**, 318–329.
20 X. M. Jiang and C. J. Brinker, *Provisional U.S. Patent* Application No. 60/903120, 2007.
21 M. Niederberger, G. Garnweitner, J. H. Ba, J. Polleux and N. Pinna, *Int. J. Nanotechnol.*, 2007, **4**, 263–281.
22 Z. S. Jing and X. M. Jiang, *Shanghai Huagong*, 1997, **22**, 6–11.
23 A. Pottier, C. Chaneac, E. Tronc, L. Mazerolles and J. P. Jolivet, *J. Mater. Chem.*, 2001, **11**, 1116–1121.
24 C. J. Homer, X. M. Jiang, T. L. Ward, C. J. Brinker and J. P. Reid, *Phys. Chem. Chem. Phys.*, 2009, **11**, 7780–7791; X. M. Jiang, T. L. Ward, F. van Swol and C. J. Brinker, Numerical Simulation on Ethanol–Water–NaCl Droplet Evaporation, *Ind. Eng. Chem. Res.*, 2010, **49**, 5631–5643.
25 A. Di Paola, M. Bellardita, R. Ceccato, L. Palmisano and F. Parrino, *J. Phys. Chem. C*, 2009, **113**, 15166–15174.
26 M. Koelsh, S. Cassaignon and J. P. Jolivet, *Mater. Res. Soc. Symp. Proc.*, 2004, **822**, 73.
27 D. Gomes, S. P. Nunes and K. V. Peinemann, *J. Membr. Sci.*, 2005, **246**, 13–25.